HHS Public Access

Author manuscript

Biol Psychiatry. Author manuscript; available in PMC 2023 January 01.

Sex-specific role for SLIT1 in regulating stress susceptibility

Yentl Y van der Zee[1,2], **Casey K Lardner**[2], **Eric M Parise**[2], **Philipp Mews**[2], **Aarthi Ramakrishnan**[2], **Vishwendra Patel**[2], **Collin D Teague**[2], **Marine Salery**[2], **Deena M Walker**[2,3], **Caleb J Browne**[2], **Benoit Labonté**[2,4], **Lyonna F Parise**[2], **Hope Kronman**[2], **Catherine J Penã**[2,5], **Angélica Torres-Berrío**[2], **Julia E Duffy**[2], **Laurence de Nijs**[1], **Lars M T Eijssen**[1], **Li Shen**[2], **Bart Rutten**[1], **Orna Issler**[2,†], **Eric J Nestler**[2,†]

[1]School for Mental Health and Neuroscience, Department of Psychiatry and Neuropsychology, Maastricht University, 6229 ER, Maastricht, the Netherlands

[2]Nash Family Department of Neuroscience and Friedman Brain Institute, Icahn School of Medicine at Mount Sinai, New York, NY 10029, USA

[3]Present address: Department of Behavioral Neuroscience, Oregon Health and Science University School of Medicine, Portland, OR 97239, USA

[4]Present address: Department of Psychiatry and Neurosciences, Faculty of Medicine, Université Laval, Québec, Canada

[5]Present address: Princeton Neuroscience Institute, Washington Road, Princeton, NJ 08544, USA

Abstract

Background—Major depressive disorder (MDD) is a pervasive and debilitating syndrome characterized by mood disturbances, anhedonia, and alterations in cognition. While the prevalence of MDD is twice as high for women compared to men, little is known about the molecular mechanisms that drive sex differences in depression susceptibility.

Methods—We discovered that Slit Guidance Ligand 1 (SLIT1), a secreted protein essential for axonal navigation and molecular guidance during development, is downregulated in the adult ventromedial prefrontal cortex (vmPFC) of depressed women compared to healthy controls, but not depressed men. This sex-specific downregulation of *Slit1* was also observed in vmPFC of mice exposed to chronic variable stress. To identify a causal, sex-specific role for SLIT1 in depression-related behavioral abnormalities, we performed knockdown (KD) of *Slit1* expression in vmPFC of male and female mice.

[†]Co-corresponding authors: Orna Issler, Tel: 212 659 5938, orna.issler@mssm.edu; Eric J. Nestler, Tel: 212 659 5656, eric.nestler@mssm.edu.

Disclosures

The authors report no biomedical financial interests or potential conflicts of interest.

Results—When combined with stress exposure, vmPFC *Slit1* KD reflected the human condition by inducing a sex-specific increase in anxiety- and depression-related behaviors. Further, we found that vmPFC *Slit1* KD decreased the dendritic arborization of vmPFC pyramidal neurons, and decreased the excitability of the neurons, in female mice, effects not observed in males. RNA-sequencing analysis of vmPFC after *Slit1* KD in female mice revealed an augmented transcriptional stress signature.

Conclusions—Together, our findings establish a crucial role for SLIT1 in regulating neurophysiological and transcriptional responses to stress within the female vmPFC, and provide mechanistic insight into novel signaling pathways and molecular factors influencing sex differences in depression susceptibility.

Keywords

Major depressive disorder; SLIT1; chronic variable stress; prefrontal cortex; RNA sequencing

Introduction

Major depressive disorder (MDD) is a highly prevalent and debilitating syndrome characterized by mood changes, an inability to feel pleasure, and alterations in physiological functions, cognition, and psychomotor activity (1). Depression is caused by a complex interplay between genetic, epigenetic, and environmental factors, and its multifaceted nature has made the identification of genes contributing to depression susceptibility difficult to identify. Further confounding this complexity is the fact that susceptibility to MDD is associated with a striking sex difference: women are affected at twice the rate of men (2-4). Furthermore, men and women tend to display a distinct presentation of depression (5), with women on average having an earlier age of onset, longer depressive episodes, heightened symptom severity, and tendency to respond to different pharmacological treatments (6). In addition, females display higher rates of comorbid anxiety disorders, while males exhibit more comorbid substance use disorders (7). While the predominance of women suffering from MDD is well-established, substantially less is known about the molecular mechanisms that underlie the sex differences observed in depression risk and presentation (8).

One predominant type of neuroadaptation in response to stress is structural changes within the cerebral cortex, including dendritic remodeling, synaptic turnover, and neuronal replacement. These adaptations have been implicated as part of structural manifestations of the depressed brain (9). Postmortem studies report a decrease in synapse numbers in medial prefrontal cortex (mPFC) of subjects suffering from depression (9). Preclinical studies extend these findings, demonstrating reductions in dendritic complexity and spine density within mPFC and hippocampus in response to chronic stress (10, 11). Atrophy of mPFC pyramidal neurons is observed after even short periods of stress (12-14), indicating that these cells are especially sensitive to environmental insult. The majority of these studies have been conducted in male rodents. However, stress has been shown to promote dynamic changes in the neuronal dendritic tree in a sex-specific manner (15). Specifically in mPFC pyramidal neurons, stress induces opposing effects on apical dendritic length in male vs. female rats (16). Yet, the molecular mechanisms by which stress causes these sex-specific structural alterations in mPFC remain poorly understood.

Guidance cues, including the Slit, Netrin, and Semaphorin families, determine the fine organization of neuronal circuits during embryonic and postnatal development (17), and are being increasingly recognized as potential targets for neurological and psychiatric disorders, including depression (18-20). One molecular pathway that has been associated with neuronal plasticity in the developing brain is the SLIT/ROBO pathway (21-24). Slit Guidance Ligands (SLIT1, SLIT2, SLIT3) are evolutionary conserved secreted glycoproteins that are implicated in axonal navigation and molecular guidance in cellular migration during neural development (25-27). SLIT1, the family member most highly expressed in the central nervous system, has been shown to positively regulate dendritic growth in cortical cells *in vitro* (28). Although SLIT/ROBO signaling has been well-characterized in neuronal development, the role for SLIT1 in regulating plastic changes during adulthood or in response to stress have not been explored.

Here, we examined how SLIT1 function within mPFC contributes to stress susceptibility and MDD in a sex-specific manner. We first identify downregulation of *Slit1* mRNA expression in the ventral mPFC (vmPFC), specifically in females, induced by chronic stress in mice and depression in humans. We then demonstrate that *Slit1* KD in mouse vmPFC promotes behavioral susceptibility to stress, leads to sex-specific alterations in dendritic morphology and excitability of vmPFC pyramidal neurons, and is linked to genome-wide changes in gene expression by RNA-sequencing (RNA-seq). Overall, these investigations highlight a novel contribution of SLIT1 to stress responses and provide further insight into understanding the signaling pathways and molecular factors that contribute to sex differences in stress susceptibility and MDD.

Methods

See supplemental information for detailed Methods.

Human brain postmortem tissue

Human postmortem brain tissue and RNA-seq data from MDD and control subjects were collected, analyzed, and reported as part of a published study (29).

Animals

C57BL/6J female or male mice were used for all experiments.

Electrophysiology

Recordings were performed on vmPFC GFP-positive cells the day after miR-*LacZ* or miR-*Slit1* infection. mEPSC peak amplitudes and interevent intervals were collected.

Dendritic morphology

Brains were collected four days after miR-*LacZ* or miR-*Slit1* infection. GFP-positive pyramidal cells within layer II-III of the vmPFC were stained and manually traced.

RNA sequencing and data analysis

Using 7 individual female mice per group, library preparation and RNA-seq were performed according to previously described methods (30).

Statistical analysis

GraphPad Prism 8.0 software package was used for analyzing the data.

Results

Female-specific downregulation of *Slit1* in vmPFC of MDD patients and chronically stressed mice

To identify sex-specific gene targets in the SLIT/ROBO pathway regulated in depression, we leveraged RNA-seq datasets previously generated by our laboratory from human depressed subjects and chronically stressed mice. The human dataset includes the transcriptomes of postmortem ventral medial prefrontal cortex (vmPFC), dorsolateral PFC (dlPFC), orbitofrontal cortex (OFC), nucleus accumbens (NAc), anterior insula (aINS), and ventral subiculum (vSUB) of male and female depressed and control human subjects (29). From this dataset, we identified a female-specific downregulation of *Slit1* mRNA in vmPFC of depressed subjects compared to controls, with no change observed in any other brain region (Fig. 1A). Notably, in control subjects there was a trend for higher levels of *Slit1* mRNA in vmPFC of females compared to males (Suppl. Fig. 1A). No other *Slit* or *Robo* family member displayed significantly altered expression in vmPFC of depressed females or males, and minimal regulation of these genes was apparent in the other brain regions studied (Suppl. Fig. 1B).

We next examined whether this sex-specific regulation of *Slit1* is also observed in mice subjected to chronic stress. To that end, we used a previously generated dataset that employed a 21-day chronic variable stress (CVS) procedure, a model well-known to induce equivalent degrees of anxiety- and depression-like behaviors in both sexes of mice as well as to mimic a subset of transcriptional abnormalities associated with human depression (29). Similar to the human findings, we identified a downregulation of *Slit1* mRNA in vmPFC of female mice exposed to CVS compared to controls, with no change seen in the NAc (Fig. 1B). There was no change in other *Slit* or *Robo* family members in either brain region (Suppl. Fig. 1C).

We confirmed these sex-specific gene expression findings by performing qPCR on the same human and mouse tissue samples used to generate the prior RNA-seq datasets (Fig. 1C,D). *Slit1* mRNA levels were significantly lower in vmPFC of female MDD patients (Two-way ANOVA, $F_{gender(1,35)}=9.7$, $p=0.0036$; $F_{disease(1,35)}=7.6$, $p=0.0088$) vs. female controls (post hoc Tukey test: $p=0.0112$). No differences were observed between male MDD and control patients. Similarly, female mice subjected to CVS displayed significantly lower levels of *Slit1* mRNA in vmPFC (Two-way ANOVA, $F_{gender(1,34)}=5.4$, $p=0.0256$; $F_{disease(1,34)}=9.3$, $p=0.0044$) compared to unstressed females (post hoc Tukey test: $p=0.0227$), whereas male animals exhibited no difference in *Slit1* gene expression following chronic stress. These analyses confirm that stress suppresses *Slit1* expression in a sex-specific manner.

To characterize the cell-type enrichment of *Slit1*, we explored existing datasets of cell type-specific gene expression (31,32). We identified neuronal cells as the principal cell type that exhibits high expression levels of *Slit1* mRNA in the adult human (Suppl. Fig. 2A) and mouse (Suppl. Fig. 2B) brain. We next used RNAscope® fluorescent *in-situ* hybridization (FISH) on adult vmPFC tissue of mice to examine whether *Slit1* is expressed predominantly in glutamatergic or GABAergic neurons (Fig. 1E). *Slit1* mRNA was co-expressed in cells positive for either the GABAergic marker glutamic acid decarboxylase 2 (*Gad2*) or the glutamatergic marker vesicular glutamate transporter 2 (*Slc17a6*), with a slightly higher percentage of *Gad2* positive neurons expressing *Slit1* ($t_{(9)}$=3.613, p=0.0056) (Fig. 1F). This finding is in line with reports from humans, showing equivalent expression of *Slit1* in glutamatergic and GABAergic neurons in OFC (Suppl. Fig. 2C) (33). However, we found that glutamatergic neurons expressed strikingly higher levels of *Slit1* compared to GABAergic neurons ($t_{(9)}$=5.628, p=0.0003) (Fig. 1G). This cell-type specific difference in expression is in line with a published single cell RNA-seq study from mouse somatosensory cortex, showing strong enrichment of *Slit1* in glutamatergic neurons (Suppl. Fig. 2D) (34).

Slit1 knockdown (KD) in vmPFC promotes sex-specific susceptibility to stress

To test the causal, sex-specific role of *Slit1* in depression- and anxiety-related behavioral abnormalities, we generated HSV vectors, which infect neurons selectively, expressing an artificial miRNA designed to target *Slit1* (miR-Slit1) or *LacZ* as a control (miR-*LacZ*). Infusion of miR-Slit1 into vmPFC (Fig. 2A) leads to effective KD of *Slit1* in this region of female ($t_{(33)}$=2.651, p=0.0061) (Fig. 2B) and male ($t_{(21)}$=1.782, p=0.0446) (Fig. 2C) mice. We then combined *Slit1* KD with a subthreshold (sCVS) procedure to test its ability to induce sex-specific anxiety- and depression-like behaviors. Whereas sCVS by itself is insufficient to induce stress-related behavioral abnormalities in normal animals, it can reveal altered stress susceptibility when combined with viral-mediated manipulation of specific genes (35). Due to divergent stress susceptibility at baseline, female mice were subjected to 3 days of sCVS (Fig. 2D) and male mice to 6 days of sCVS (Fig. 2E), followed by behavioral testing (35). When followed by sCVS, *Slit1* KD in female vmPFC increased latency to feed in the novelty suppressed feeding (NSF) test (Fig. 2F) (Two-way ANOVA, $F_{interaction(1,38)}$=4.110, p=0.0497; $F_{stress(1,38)}$=4.640, p=0.0376) compared to miR-*LacZ* controls (post hoc Tukey test: p=0.0415), miR-*Slit1* non-stressed mice (post hoc Tukey test: p=0.0262), and miR-*LacZ* sCVS mice (trend, post hoc Tukey test: p=0.0589). We found no differences in latency to feed in the home cage as part of the post-test (Suppl. Fig. 3A), suggesting that the effects observed in NSF are not due to alternation in appetite between the groups. Consistent with these results, miR-*Slit1* sCVS females exhibited decreased sucrose preference (SP) compared to all of the other groups (Two-way ANOVA, $F_{interaction(1,37)}$=4.781, p=0.0352; $F_{stress(1,37)}$=4.324, p=0.0446; post hoc Tukey test: miR-*Slit1* sCVS vs. miR-*LacZ* control, p=0.0429; miR-*Slit1* sCVS vs. miR-*Slit1* control, p=0.0418; miR-*Slit1* sCVS vs. miR-*Slit1* control, p=0.0249) (Fig. 2G). We observed no differences between the groups in marble burying (MB) or the forced swim test (FST) (Fig. 2H,I). By contrast, the same manipulation in combination with 6 days of sCVS did not promote susceptibility to stress in male mice in any of these tests (figure 2J-L). Male mice in the different groups had similar latencies to feed during the NSF post-test as well (Suppl. Fig. 3B). Notably, we observed increased immobility time in the FST in male mice treated

with miR-*Slit1* regardless of stress exposure ($F_{virus(1,33)}$=5.1, p=0.0297) (Fig. 2M). Together, these findings suggest that *Slit1* KD in vmPFC promotes abnormal stress responses in a sex-specific manner that mimics the human phenomena.

Slit1 KD decreases dendritic arbor length and branching and alters neurophysiological properties of vmPFC neurons of female mice

We next explored the potential mechanisms linked to the behavioral effects of *Slit1* KD. SLIT1 has been reported to alter dendritic morphology in embryonic cortical mouse neurons *in vitro* (36), but there are no reports of its influence in the adult brain. To that end, we performed immunohistochemistry on miR-*Slit1* or miR-*LacZ* infected vmPFC tissue of female adult mice. We focused our attention on pyramidal neurons from layer II/III of vmPFC, as past studies have identified these cells to be critical for modulating stress responses in mice (13,37). Figure 3A shows representative reconstructed pyramidal neurons for each group. Following miR-*Slit1* infection, pyramidal neurons displayed a robust decrease in dendritic size and branching with no change in the soma surface area compared to miR-*LacZ* controls (Suppl. Fig. 4A). The total apical dendritic arbor length ($t_{(35)}$=3.135, p=0.0035) (Fig. 3B) and branching ($t_{(36)}$=2.490, p=0.0175) (Fig. 3C) were decreased by *Slit1* KD. Similarly, *Slit1* KD decreased the total basal dendritic arbor length ($t_{(38)}$=2.486, p=0.0175) (Fig. 3D), branching ($t_{(39)}$=3.499, p=0.0012) (Fig. 3E), and average basal dendritic arbor length ($t_{(39)}$=3.896, p=0.0004) (Suppl. Fig. 4B). Scholl analysis found no difference between the two groups for apical dendritic length (Fig. 3F) or branching (Suppl. Fig. 4C), but revealed a significant reduction in the dendritic length between 60-100μm from the cell body (Fig. 3G) and the number of interactions in basal arbors (Suppl. Fig. 4D), indicating that dendritic restructuring induced by miR-*Slit1* was confined to proximal basal dendritic branches.

We repeated the same experiment in male mice. Figure 3H shows representative reconstructed pyramidal neurons for each group. Following miR-*Slit1* infection, pyramidal neurons displayed no change in the soma surface area compared to miR-*LacZ* controls (Suppl. Fig. 4E). *Slit1* KD increased the total apical dendritic arbor length in males ($t_{(34)}$=2.185, p=0.0351) (Fig. 3I). No change was seen in the total apical dendritic branching (Fig. 3J), total basal dendritic arbor length (Fig. 3K) and branching (Fig. 3L), or in the average basal dendritic length (Suppl. Fig. 4F). However, Scholl analysis revealed a significant increase in the apical dendritic length of the male miR-*Slit1* group compared to controls between 60-140μm from the soma (Fig. 3M) and the number of interactions (Suppl. Fig. 4G). In addition, between 40-100μm away from the cell body, we observed a significant increase in the basal dendritic length (Fig. 3N) and the number of interactions (Suppl. Fig. 4H) in the miR-*Slit1* group compared to the miR-*LacZ* mice. Together, these results show that *Slit1* KD leads to reduced dendritic length and branching in females, while increasing apical dendritic length in males, which confirms a sex-specific role for *Slit1* in dendritic remodeling in the rodent adult brain.

We followed up on these morphological findings by assessing the impact of *Slit1* KD on the electrophysiological properties of pyramidal neurons in vmPFC of female and male mice. We show representative mEPSC traces of vmPFC neurons after miR-*Slit1* or miR-*LacZ*

infection (Fig. 4A,B). In females, miR-*Slit1* reduced the amplitude of mEPSCs compared to miR-*LacZ* controls (Fig. 4C) per cell (Mann-Whitney U=42, n_1=17, n_2=15, p=0.0008) (Fig. 4D) and per animal (Mann-Whitney U=0, n_1=n_2=4, p=0.0286) (Fig. 4E), with no change observed in interevent interval (Fig. 4F-H). In contrast, we found no differences for male mEPSC amplitude (Fig. 4I-K), and increased interevent interval following *Slit1* KD (Fig. 4L) analyzed per cell (Mann-Whitney U=86, n_1=21, n_2=15, p=0.0213) (Fig. 4M), although this effect did not hold up when analyzed per animal (Fig. 4N). Together, these results demonstrate that *Slit1* KD alters synaptic function of adult vmPFC pyramidal neurons in a sex-specific fashion, which may contribute to aberrant behavioral responses to stress.

Slit1 KD enhances stress-induced transcriptional activation

Next, we used RNA-seq to explore the molecular mechanisms by which *Slit1* controls neuronal morphology, physiology, and stress-related behavior. We surveyed genome-wide transcriptional changes in female mouse vmPFC tissue after miR-*Slit1* or miR-*LacZ* infection at baseline or after sCVS (Fig. 5A). Analysis of differentially expressed genes (DEGs), using cutoff: p<0.05 and fold-change>30%, showed that *Slit1* KD in vmPFC neurons alone increased the expression of 172 genes and reduced expression levels of 117 genes (Fig. 5B). In combination with sCVS, *Slit1* KD increased the expression of several-fold more genes with only modest increases in the number of downregulated transcripts. The union heatmaps presented in Figure 5C confirms an enhanced transcriptional upregulation in response to sCVS in the *Slit1* KD condition compared to LacZ controls. Gene ontology (GO) analysis revealed that the DEGs in the miR-*LacZ* sCVS group were enriched for biological processes related to hormonal responses, such as estrogen biosynthesis and androgen metabolism, while the miR-*Slit1* sCVS group terms were directly relating to known functions of SLIT1, including extracellular matrix organization (38,39) and collagen fibril organization (40) (Fig. 5D). Notably, miR-*Slit1* followed by subthreshold stress alters a large subset of genes related to different aspects of synaptic functioning (Suppl. Table 3).

We performed Ingenuity Pathway Analysis (IPA) to identify predicted transcriptional upstream drivers of the genes regulated by *Slit1* manipulation (Suppl. Table 4). We identified *Ccnd1*, encoding the cell cycle regulatory protein cyclin D1 (41), as the highest-ranked upstream regulator for the miR-*Slit1* sCVS vs. baseline DEG list (Fig. 5E). In contrast, *Ccnd1* was not a predicted regulator of the DEGs for the miR-*LacZ* sCVS vs. baseline comparison. Our IPA analysis also predicted that *Ccnd1* is upregulated in the miR-*Slit1* sCVS condition (Fig. 5F). Indeed, we found that *Ccnd1* mRNA levels are significantly upregulated in our miR-*Slit1* sCVS vs. baseline RNA-seq data. Additionally, of the genes predicted to be regulated by *Ccnd1*, 38 are differentially expressed within our miR-*Slit1* sCVS vs. baseline comparison (Fig. 5G). Interestingly, however, *Ccnd1* expression is not altered in vmPFC in human depression or mouse CVS (data not shown). Together, these results suggest that *Slit1* KD alters behavioral and neurophysiological responses to stress potentially through modulation of CCND1 signaling pathways.

Discussion

Our current understanding of the molecular mechanisms leading to an increased depression risk in women is limited. Previously, our laboratory reported that the molecular abnormalities associated with MDD are strikingly divergent between males and females, with limited overlap of transcriptome changes in the two sexes (29), a finding replicated by another group in an independent cohort (42). The present study identified *Slit1* as a sex-specific target that is linked to female MDD risk. We show that this neuronal-enriched gene is downregulated in vmPFC of female, but not male, MDD patients and, likewise, is lowered in vmPFC of female and not male mice after CVS. This pattern can be interpreted as masculinization of *Slit1* expression by stress and depression given the higher basal levels of *Slit1* seen in normal females. We go on to demonstrate that viral-mediated *Slit1* KD in vmPFC neurons promotes behavioral sensitivity to stress in a sex-specific manner: females display increased depressive- and anxiety-like behaviors in the NSF and SP tests. In contrast, male mice did not show behavioral differences in these tests upon *Slit1* KD, but exhibited increased immobility in the FST. This result might relate to sex differences in depression symptoms (5), in which women report higher levels of comorbid anxiety compared to males (7). We demonstrate further in female mice that *Slit1* KD alters synaptic physiology and leads to shrinking of dendritic trees of vmPFC pyramidal neurons, as well as augments the effects of stress on gene expression on a genome-wide scale. Together, this work identifies *Slit1* as a novel target in MDD and provides insight into signaling pathways and molecular factors contributing to sex differences in depression and stress susceptibility. As well, this study is another example that, despite the highly heterogeneous and complex nature of MDD, manipulating a single target gene in mouse mPFC can alter behavioral responses to stress in a sex-specific fashion (30,35).

SLIT1 has been found to increase the growth and branching of mouse cortical dendrites *in vitro* (36). As dendritic branching and synaptic plasticity are critical for learned responses to stress and other environmental factors (43), we investigated whether *Slit1* manipulation affects the dendritic structure of vmPFC pyramidal neurons. Our morphological data show that KD of *Slit1* decreases arbor length and branching of the apical and basal dendrites of these neurons in female mice. In contrast, we found increased apical arbor length in male mice. These results thereby confirmed a sex-specific role for *Slit1* in regulating dendritic morphology in the adult mouse brain. The apical and basal dendrites of pyramidal neurons in PFC occupy distinct cortical layers, and receive information from axons originating from distinct cortical brain regions (44). Whereas the apical tuft is thought to integrate feedback information, the basal dendrites receive feedforward sensory input (45), which allows the pyramidal neurons to integrate separate sets of inputs independently. Maintaining the right balance is essential for the proper relay of cortical information processing. The loss of branching and elongation at the level of dendrites may lead to inadequate responses to environmental stimuli, which could affect neuronal plasticity and leave female mice more susceptible to stress (10).

Previous studies, predominantly conducted in male rodents, have shown that chronic stressors were capable of inducing atrophy of apical and basal dendrites in layer II-III mPFC pyramidal neurons (12,46,47). However, a recent study demonstrated that repeated stress

decreased branching of layer II/III apical dendrites in vmPFC of both male and female rats (48). Other studies have shown sex-specific results following stress. For example, Garrett et al. showed that chronic stress decreased apical dendritic branch number and length of male rat pyramidal neurons in PFC, whereas the same stressors increased apical dendritic length in female rats (16). Similarly, social instability stress during adolescence reduced apical length in female rats, while reducing basilar length in males (49). These findings along with ours highlight the need for future studies systematically testing the effects of different types of stressors during different developmental windows on dendritic morphology, as well as spine volume and number, in both sexes.

Dysregulation of synaptic plasticity in mPFC has been implicated as a sex-specific process in MDD (50). Our data show that glutamatergic neurons expressed many-fold higher levels of *Slit1* compared to GABAergic neurons, and that *Slit1* KD decreases the branching of pyramidal cell dendrites in vmPFC of female mice. We therefore tested whether KD of *Slit1* also alters the excitability of these cells. Our analysis of postsynaptic currents revealed that *Slit1* KD significantly lowered the amplitude of mEPSCs, which suggests postsynaptic changes. Similarly, inhibition of miR-214-3p in mPFC reversed depressive-like behavior in male mice that underwent chronic social defeat, a finding that was accompanied by an increase in mEPSC amplitude and number of dendritic spines (51). The synaptic changes caused by *Slit1* KD are consistent with the changes we observed in dendrite morphology. The synaptic changes might be related to the wide range of synaptic proteins whose mRNA expression levels are altered upon *Slit1* KD in vmPFC in our RNA-seq dataset. Additionally, given that *Slit1* is expressed in GABAergic neurons as well, future studies should explore the effects of *Slit1* KD on inhibitory postsynaptic currents and excitatory/inhibitory balance.

To examine the underlying molecular contributions to the observed changes in vmPFC morphology and function, we performed RNA-seq after *Slit1* KD. This analysis revealed that *Slit1* KD augments expression of genes that are induced by sCVS. Further, reduction of *Slit1* regulates DEGs that relate directly to the functioning of the SLIT/ROBO pathway, such as extracellular matrix organization (38,39) and collagen fibril organization (40). Our findings implicate *Ccnd1*, encoding cyclin D1 (41), as a major driver of the transcriptional changes following *Slit1* KD in female vmPFC. Cyclin D1, which is expressed in the cortex of the adult brain (52), belongs to the conserved cyclin-dependent kinase (CDK) family which drives transitions through cell cycles and cell proliferation (53). In line with our findings, CCND1 has been shown to regulate neuronal morphology and the organization of dendritic trees during development (54). Additionally, CCND1 is upregulated in the amygdala following stress (55). SLIT/ROBO are suggested to influence members of the RHO GTPase family, such as RHOA, which are key regulators of the actin cytoskeletal and neuronal morphology (56). Interestingly, there is evidence that CCND1 acts as an effector of RHOA (57,58). In our miR-*Slit1* sCVS vs. baseline comparison, RHOA was also identified as a predicted upstream regulator of *Ccnd1*. While *Ccnd1* was not altered in our human MDD or mouse CVS data sets (29), it was upregulated following a subthreshold stress paradigm in combination with *Slit1* KD. This suggests that *Ccnd1* may play a molecular role in the initial acute stress phase in females. Together, we hypothesize that the CCND1 pathway activated by RHOA as a result of *Slit1* downregulation in the adult female vmPFC contributes to reduced dendritic branching as part of the molecular, morphological, and

physiological changes leading to increased susceptibility to stress and depression. In this vein, it is interesting to note that, while SLIT1 is expressed predominantly in neurons, CCND1 is expressed predominantly in non-neuronal cells, which highlights bidirectional, inter-cellular communication as a key pathophysiological mechanism for stress-related disorders.

To conclude, this study implicates a role for SLIT1 in the adult brain and in MDD, and provides new insight into the growing field that recognizes the potential of axon guidance molecules as targets for adult neurological and psychiatric disorders such as depression. Further experiments are needed to extend our work to investigate the mechanisms that underlie the sex-specific effects observed in our study. Nevertheless, our findings shed light on a novel signaling pathway and its molecular constituents for the development of innovative treatments for MDD.

Supplementary Material

Refer to Web version on PubMed Central for supplementary material.

Acknowledgments

This work was funded by R01MH051399 and P50MH096890 and by the Hope for Depression Research Foundation (HDRF). We wish to thank Robert Blitzer and Amanda Fakira from Mount Sinai's electrophysiology core facility; Bridget Wicinski, Merina Varghese, and Patrick Hof for their training in dendritic morphology analysis; John Kutlu and James Simpson for their graphical training; and Hilde Schot for her never ending support.

References

1. Fava M, Kendler KS. Major Depression Disorder Neuron. 2000;28(2):335–41. [PubMed: 11144343]
2. Kessler RC. Epidemiology of women and depression. Journal of Affective Disorders. 2003;74(1):5–13. [PubMed: 12646294]
3. Kessler RC, Chiu WT, Demler O, Merikangas KR, Walters EE. Prevalence, severity, and comorbidity of 12-month DSM-IV disorders in the National Comorbidity Survey Replication. Arch Gen Psychiatry. 2005;62:617–27. [PubMed: 15939839]
4. Kuehner C Gender differences in unipolar depression: an update of epidemiological findings and possible explanations. . Acta Psychiatr Scand. 2003;108:163–74. [PubMed: 12890270]
5. Sramek JJ, Murphy MF, Cutler NR. Sex differences in the psychopharmacological treatment of depression. Dialogues Clin Neurosci. 2016;18(4):447–57. [PubMed: 28179816]
6. Marcus SM, Young EA, Kerber KB, Kornstein S, Farabaugh AH, Mitchell J, et al. Gender differences in depression: findings from the STAR*D study. J Affect Disord. 2005;87(2-3):141–50. [PubMed: 15982748]
7. Marcus SM, Kerber KB, Rush AJ, Wisniewski SR, Nierenberg A, Balasubramani GK, et al. Sex differences in depression symptoms in treatment-seeking adults: confirmatory analyses from the Sequenced Treatment Alternatives to Relieve Depression study. Compr Psychiatry. 2008;49(3):238–46. [PubMed: 18396182]
8. Issler O, Nestler EJ. The molecular basis for sex differences in depression susceptibility. Current Opinion in Behavioral Sciences 2018. p. 1–6.
9. Kang HJ, Voleti B, Hajszan T, Rajkowska G, Stockmeier CA, Licznerski P, et al. Decreased expression of synapse-related genes and loss of synapses in major depressive disorder. Nat Med. 2012;18(9):1413–7. [PubMed: 22885997]
10. McEwen BS, Eiland L, Hunter RG, Miller MM. Stress and anxiety: structural plasticity and epigenetic regulation as a consequence of stress. Neuropharmacology. 2012;62(1):3–12. [PubMed: 21807003]

11. Hare BD, Duman RS. Prefrontal cortex circuits in depression and anxiety: contribution of discrete neuronal populations and target regions. Mol Psychiatry. 2020.
12. Brown SM, Henning S, Wellman CL. Mild, short-term stress alters dendritic morphology in rat medial prefrontal cortex. Cereb Cortex. 2005;15(11):1714–22. [PubMed: 15703248]
13. Izquierdo A, Wellman CL, Holmes A. Brief uncontrollable stress causes dendritic retraction in infralimbic cortex and resistance to fear extinction in mice. J Neurosci. 2006;26(21):5733–8. [PubMed: 16723530]
14. Kim H, Yi JH, Choi K, Hong S, Shin KS, Kang SJ. Regional differences in acute corticosterone-induced dendritic remodeling in the rat brain and their behavioral consequences. BMC Neurosci. 2014;15:65. [PubMed: 24884833]
15. McEwen BS, Nasca C, Gray JD. Stress Effects on Neuronal Structure: Hippocampus, Amygdala, and Prefrontal Cortex. Neuropsychopharmacology. 2016;41(1):3–23. [PubMed: 26076834]
16. Garrett JE, Wellman CL. Chronic stress effects on dendritic morphology in medial prefrontal cortex: sex differences and estrogen dependence. Neuroscience. 2009;162(1):195–207. [PubMed: 19401219]
17. Chédotal A, Richards LJ. Wiring the brain: the biology of neuronal guidance. Cold Spring Harb Perspect Biol. 2010;2(6):a001917. [PubMed: 20463002]
18. Van Battum EY, Brignani S, Pasterkamp RJ. Axon guidance proteins in neurological disorders. Lancet Neurol. 2015;14(5):532–46. [PubMed: 25769423]
19. Torres-Berrío A, Lopez JP, Bagot RC, Nouel D, Dal Bo G, Cuesta S, et al. DCC Confers Susceptibility to Depression-like Behaviors in Humans and Mice and Is Regulated by miR-218. Biol Psychiatry. 2017;81(4):306–15. [PubMed: 27773352]
20. Torres-Berrío A, Hernandez G, Nestler EJ, Flores C. The Netrin-1/DCC Guidance Cue Pathway as a Molecular Target in Depression: Translational Evidence. Biol Psychiatry. 2020.
21. Brose K, Bland KS, Wang KH, Arnott D, Henzel W, Goodman CS, et al. Slit proteins bind Robo receptors and have an evolutionarily conserved role in repulsive axon guidance. Cell. 1999;96(6):795–806. [PubMed: 10102268]
22. Kidd T, Bland KS, Goodman CS. Slit is the midline repellent for the robo receptor in Drosophila. Cell. 1999;96(6):785–94. [PubMed: 10102267]
23. Li HS, Chen JH, Wu W, Fagaly T, Zhou L, Yuan W, et al. Vertebrate slit, a secreted ligand for the transmembrane protein roundabout, is a repellent for olfactory bulb axons. Cell. 1999;96(6):807–18. [PubMed: 10102269]
24. Blockus H, Chédotal A. Slit-Robo signaling. Development. 2016;143(17):3037–44. [PubMed: 27578174]
25. Marin O, Plump AS, Flames N, Sanchez-Camacho C, Tessier-Lavigne M, Rubenstein JL. Directional guidance of interneuron migration to the cerebral cortex relies on subcortical Slit1/2-independent repulsion and cortical attraction. Development. 2003;130(9):1889–901. [PubMed: 12642493]
26. Nguyen-Ba-Charvet KT, Picard-Riera N, Tessier-Lavigne M, Baron-Van Evercooren A, Sotelo C, Chedotal A. Multiple roles for slits in the control of cell migration in the rostral migratory stream. J Neurosci. 2004;24(6):1497–506. [PubMed: 14960623]
27. Xiao T, Staub W, Robles E, Gosse NJ, Cole GJ, Baier H. Assembly of lamina-specific neuronal connections by slit bound to type IV collagen. Cell. 2011;146(1): 164–76. [PubMed: 21729787]
28. Lin S-H, Chen W-C, Lu K-H, Chen P-J, Hsieh S-C, Pan T-M, et al. Down-regulation of Slit–Robo Pathway Mediating Neuronal Cytoskeletal Remodeling Processes Facilitates the Antidepressive-like Activity of Gastrodia elata Blume. J Agric Food Chem. 2014;62(43):10493–503. [PubMed: 25197951]
29. Labonté B, Engmann O, Purushothaman I, Menard C, Wang J, Tan C, et al. Sex-specific transcriptional signatures in human depression. Nat Med. 2017;23(9):1102–11. [PubMed: 28825715]
30. Issler O, van der Zee YY, Ramakrishnan A, Wang J, Tan C, Loh YE, et al. Sex-Specific Role for the Long Non-coding RNA LINC00473 in Depression. Neuron. 2020;106(6):912–26.e5. [PubMed: 32304628]

31. Zhang Y, Chen K, Sloan SA, Bennett ML, Scholze AR, O'Keeffe S, et al. An RNA-sequencing transcriptome and splicing database of glia, neurons, and vascular cells of the cerebral cortex. J Neurosci. 2014;34(36):11929–47. [PubMed: 25186741]
32. Zhang Y, Sloan SA, Clarke LE, Caneda C, Plaza CA, Blumenthal PD, et al. Purification and Characterization of Progenitor and Mature Human Astrocytes Reveals Transcriptional and Functional Differences with Mouse. Neuron. 2016;89(1):37–53. [PubMed: 26687838]
33. Kozlenkov A, Wang M, Roussos P, Rudchenko S, Barbu M, Bibikova M, et al. Substantial DNA methylation differences between two major neuronal subtypes in human brain. Nucleic Acids Res. 2016;44(6):2593–612. [PubMed: 26612861]
34. Zeisel A, Muñoz-Manchado AB, Codeluppi S, Lönnerberg P, La Manno G, Juréus A, et al. Brain structure. Cell types in the mouse cortex and hippocampus revealed by single-cell RNA-seq. Science. 2015;347(6226):1138–42. [PubMed: 25700174]
35. Hodes GE. Sex differences in nucleus accumbens transcriptome profiles associated with susceptibility versus resilience to sub-chronic variable stress. Journal of Neuroscience. 2015;35(50):16362–76. [PubMed: 26674863]
36. Whitford KL, Marillat V, Stein E, Goodman CS, Tessier-Lavigne M, Chedotal A, et al. Regulation of cortical dendrite development by Slit-Robo interactions. Neuron. 2002;33(1):47–61. [PubMed: 11779479]
37. Shrestha P, Mousa A, Heintz N. Layer 2/3 pyramidal cells in the medial prefrontal cortex moderate stress induced depressive behaviors. Elife. 2015;4.
38. Rothberg JM, Jacobs JR, Goodman CS, Artavanis-Tsakonas S. slit: an extracellular protein necessary for development of midline glia and commissural axon pathways contains both EGF and LRR domains. Genes Dev. 1990;4(12A):2169–87. [PubMed: 2176636]
39. Bhat KM. Post-guidance signaling by extracellular matrix-associated Slit/Slit-N maintains fasciculation and position of axon tracts in the nerve cord. PLoS Genet. 2017;13(11):e1007094. [PubMed: 29155813]
40. Liu J, Zhang L, Wang D, Shen H, Jiang M, Mei P, et al. Congenital diaphragmatic hernia, kidney agenesis and cardiac defects associated with Slit3-deficiency in mice. Mech Dev. 2003;120(9):1059–70. [PubMed: 14550534]
41. Bartkova J, Lukas J, Müller H, Lützhøft D, Strauss M, Bartek J. Cyclin D1 protein expression and function in human breast cancer. Int J Cancer. 1994;57(3):353–61. [PubMed: 8168995]
42. Seney ML, Huo Z, Cahill K, French L, Puralewski R, Zhang J, et al. Opposite Molecular Signatures of Depression in Men and Women. Biol Psychiatry. 2018;84(1):18–27. [PubMed: 29548746]
43. Duman RS, Aghajanian GK, Sanacora G, Krystal JH. Synaptic plasticity and depression: new insights from stress and rapid-acting antidepressants. Nat Med. 2016;22(3):238–49. [PubMed: 26937618]
44. Spratling MW. Cortical region interactions and the functional role of apical dendrites. Behav Cogn Neurosci Rev. 2002;1(3):219–28. [PubMed: 17715594]
45. Larkum M A cellular mechanism for cortical associations: an organizing principle for the cerebral cortex. Trends Neurosci. 2013;36(3):141–51. [PubMed: 23273272]
46. Radley JJ, Sisti HM, Hao J, Rocher AB, McCall T, Hof PR, et al. Chronic behavioral stress induces apical dendritic reorganization in pyramidal neurons of the medial prefrontal cortex. Neuroscience. 2004;125(1):1–6. [PubMed: 15051139]
47. Cerqueira JJ, Taipa R, Uylings HB, Almeida OF, Sousa N. Specific configuration of dendritic degeneration in pyramidal neurons of the medial prefrontal cortex induced by differing corticosteroid regimens. Cereb Cortex. 2007;17(9):1998–2006. [PubMed: 17082516]
48. Urban KR, Geng E, Bhatnagar S, Valentino RJ. Age- and sex-dependent impact of repeated social stress on morphology of rat prefrontal cortex pyramidal neurons. Neurobiol Stress. 2019;10:100165. [PubMed: 31193524]
49. Breach MR, Moench KM, Wellman CL. Social instability in adolescence differentially alters dendritic morphology in the medial prefrontal cortex and its response to stress in adult male and female rats. Dev Neurobiol. 2019;79(9-10):839–56. [PubMed: 31612626]

50. Christoffel DJ, Golden SA, Russo SJ. Structural and synaptic plasticity in stress-related disorders. Rev Neurosci. 2011;22(5):535–49. [PubMed: 21967517]
51. Deng ZF, Zheng HL, Chen JG, Luo Y, Xu JF, Zhao G, et al. miR-214-3p Targets β-Catenin to Regulate Depressive-like Behaviors Induced by Chronic Social Defeat Stress in Mice. Cereb Cortex. 2019;29(4):1509–19. [PubMed: 29522177]
52. Uhlén M, Fagerberg L, Hallström BM, Lindskog C, Oksvold P, Mardinoglu A, et al. Proteomics. Tissue-based map of the human proteome. Science. 2015;347(6220):1260419. [PubMed: 25613900]
53. Qie S, Diehl JA. Cyclin D1, cancer progression, and opportunities in cancer treatment. J Mol Med (Berl). 2016;94(12):1313–26. [PubMed: 27695879]
54. Pogoriler J, Millen K, Utset M, Du W. Loss of cyclin D1 impairs cerebellar development and suppresses medulloblastoma formation. Development. 2006;133(19):3929–37. [PubMed: 16943274]
55. Cong M, Wen L, Han F, Xu Y, Shi Y. Alterations in cyclin D1 and cyclin-dependent kinase 4 expression in the amygdalae of post-traumatic stress disorder rats. Mol Med Rep. 2017;16(6):8351–8. [PubMed: 28983608]
56. Blockus H, Chédotal A. The multifaceted roles of Slits and Robos in cortical circuits: from proliferation to axon guidance and neurological diseases. Curr Opin Neurobiol. 2014;27:82–8. [PubMed: 24698714]
57. Keely PJ. Rho GTPases as early markers for tumour progression. Lancet. 2001;358(9295):1744–5. [PubMed: 11734226]
58. Watts KL, Cottrell E, Hoban PR, Spiteri MA. RhoA signaling modulates cyclin D1 expression in human lung fibroblasts; implications for idiopathic pulmonary fibrosis. Respir Res. 2006;7:88. [PubMed: 16776827]

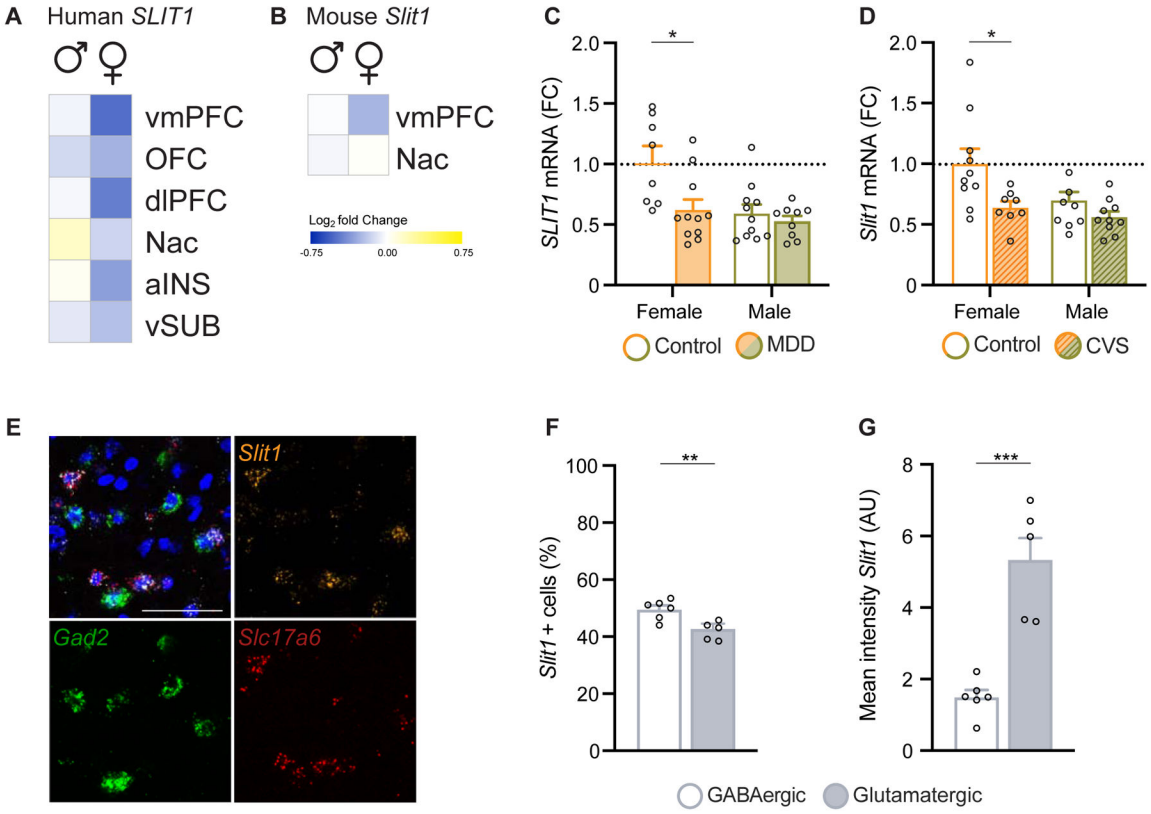

Figure 1. Neuronal *Slit1* is downregulated in the vmPFC of depressed human females and chronically stressed female mice.

(A) Heatmap representing RNA-seq results indicating *Slit1* downregulation in the vmPFC of depressed females, but not males, compared to control. vmPFC, ventromedial prefrontal cortex; dlPFC, dorsolateral PFC; OFC, orbitofrontal cortex; NAc, nucleus accumbens; aINS, anterior insula; and vSUB, ventral subiculum. **(B)** Heatmap representing RNA-seq results indicating *Slit1* mRNA downregulation in the vmPFC of female, but not male, mice after chronic variable stress (CVS). **(C)** Bar graph showing qPCR validation of *Slit1* mRNA downregulation in vmPFC of depressed females only (n=8-11/group). **(D)** Bar graph showing qPCR validation of *Slit1* mRNA downregulation after CVS in female mice only (n=8-10/group). **(E)** Representative vmPFC images from FISH for *Slit1* (orange), *Gad2* (GABAergic marker, green) and *Scl17a6* (glutamatergic marker, red) mRNA (scale bars, 50 μm). **(F)** Quantification of FISH images indicates that *Slit1* is expressed in both glutamatergic and GABAergic neurons with slightly higher co-localization in *Gad2* expressing cells (n=5-6 animals). **(G)** Quantification of *Slit1* mRNA shows markedly higher expression levels per cell in glutamatergic neurons compared to GABAergic neurons (n=5-6 animals). *p<0.05, **p<0.01, ***p<0.001. Data are shown as mean ± s.e.m.

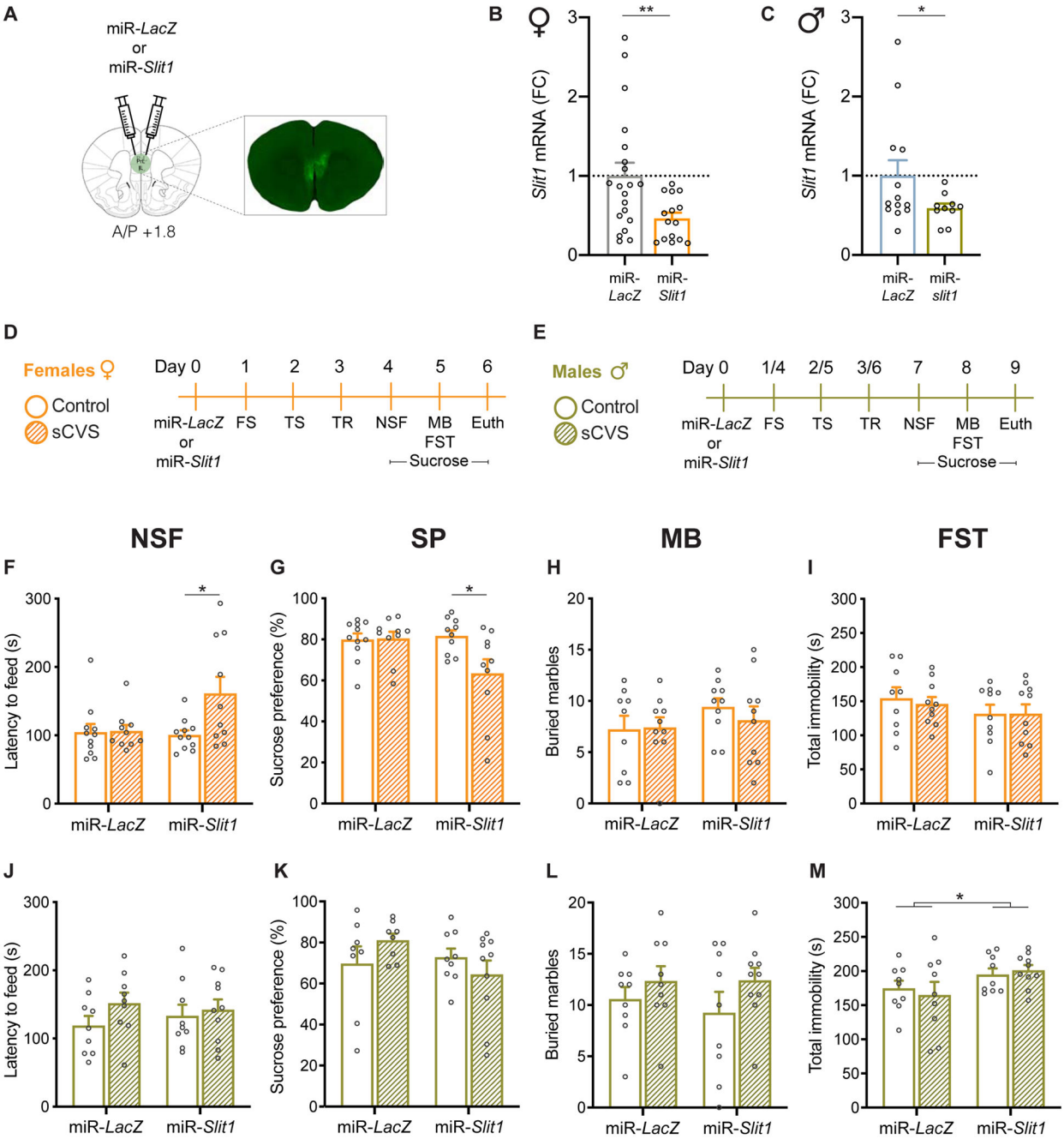

Figure 2. *Slit1* KD in vmPFC neurons controls a sex-specific anxiety- and depression-like phenotype in mice.

(A) Schematic representation of viral delivery to KD *Slit1* in mouse vmPFC. **(B, C)** Quantification of HSV-mediated knockdown of *Slit1* in the vmPFC validates significant downregulation in female **(B)** and male **(C)** mice (n=10-20). **(D, E)** Schematic representation of the experimental design in female **(D)** or male mice **(E)** including surgery, exposure to subthreshold chronic variable stress (sCVS), and behavioral tests used to assess the impact of *Slit1* KD compared to controls. **(F, J)** *Slit1* KD in the female vmPFC followed by sCVS increased latency to feed in the novelty suppressed feeding (NSF) test compared

to their unstressed counterparts as well as unstressed controls **(F)**, but had no effect in males **(J)**. **(G, K)** miR-*Slit1* sCVS females consumed less sucrose as measured in the sucrose preference (SP) test compared to all the other groups **(G)**, with no effects observed in males **(K)**. **(H, L)** No differences in the marble burying (MB) test in both females (**H)** and males **(L)**. **(I, M)** No differences in the forced swim test (FST) in females **(I)**, but increased immobility time in *miR-Slit1* males compared to controls. **(M)**. *p<0.05. Data are shown as means ± s.e.m.

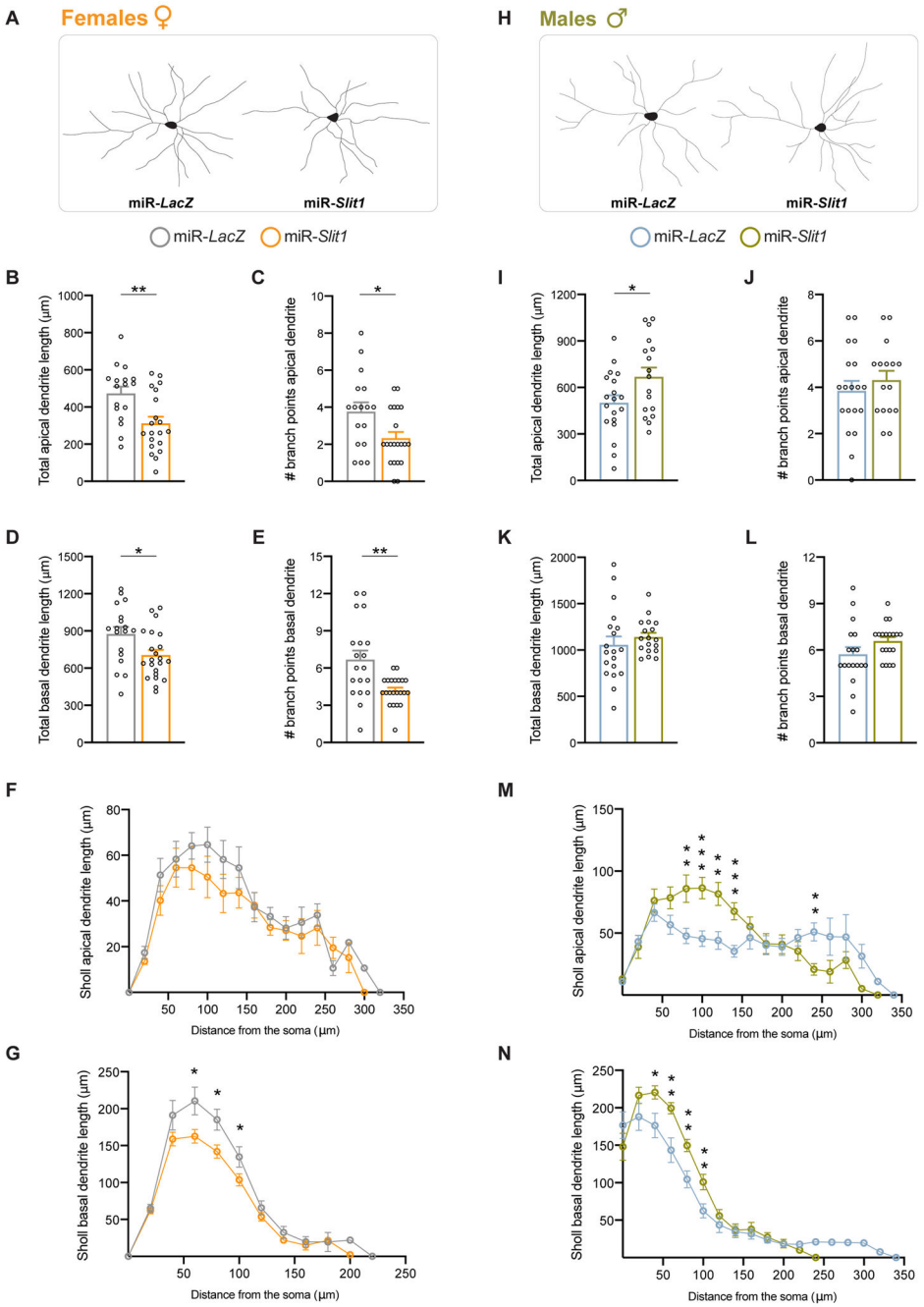

Figure 3. *Slit1* KD affects dendritic arbor length and branching in vmPFC pyramidal neurons of in a sex-specific manner.

(A) Representative tracings of pyramidal neurons in the vmPFC of female mice after miR-*LacZ* (left) or miR-*Slit1* infection (right). **(B, C)** Total apical dendritic arbor length **(B)** and branching **(C)** were decreased after miR-*Slit1* infection when compared to miR-*LacZ* controls. **(D, E)** *Slit1* KD decreased the total basal dendritic arbor length **(D)** and number of branches **(E)** compared to controls (n=82-83 dendrites/group). **(F, G)** Scholl analysis revealed no change in length of apical dendrites in vmPFC pyramidal neurons infected with miR-*Slit1* compared to miR-*LacZ* **(F)**, but a decrease in the length **(G)** of basal dendrites

mainly 60-100 μm from the soma. **(H)** Representative tracings of pyramidal neurons in the vmPFC of male mice after miR-*LacZ* (left) or miR-*Slit1* infection (right). **(I)** Total apical dendritic arbor was increased after miR-*Slit1* infection when compared to miR-*LacZ* controls. **(J-L)** No change was observed in apical branching **(J)**, the total basal dendritic arbor length **(K)** or number of branches **(L)** compared to controls (n=85-91 dendrites/group). **(M, N)** Scholl analysis revealed an increase in the length of apical **(M)** and basal **(N)** dendrites mainly 80-140 μm from the soma. Per group: n=5 animals, 19-22 neurons. *p<0.05, **p<0.01, ***p<0.001. Data are shown as means ± s.e.m.

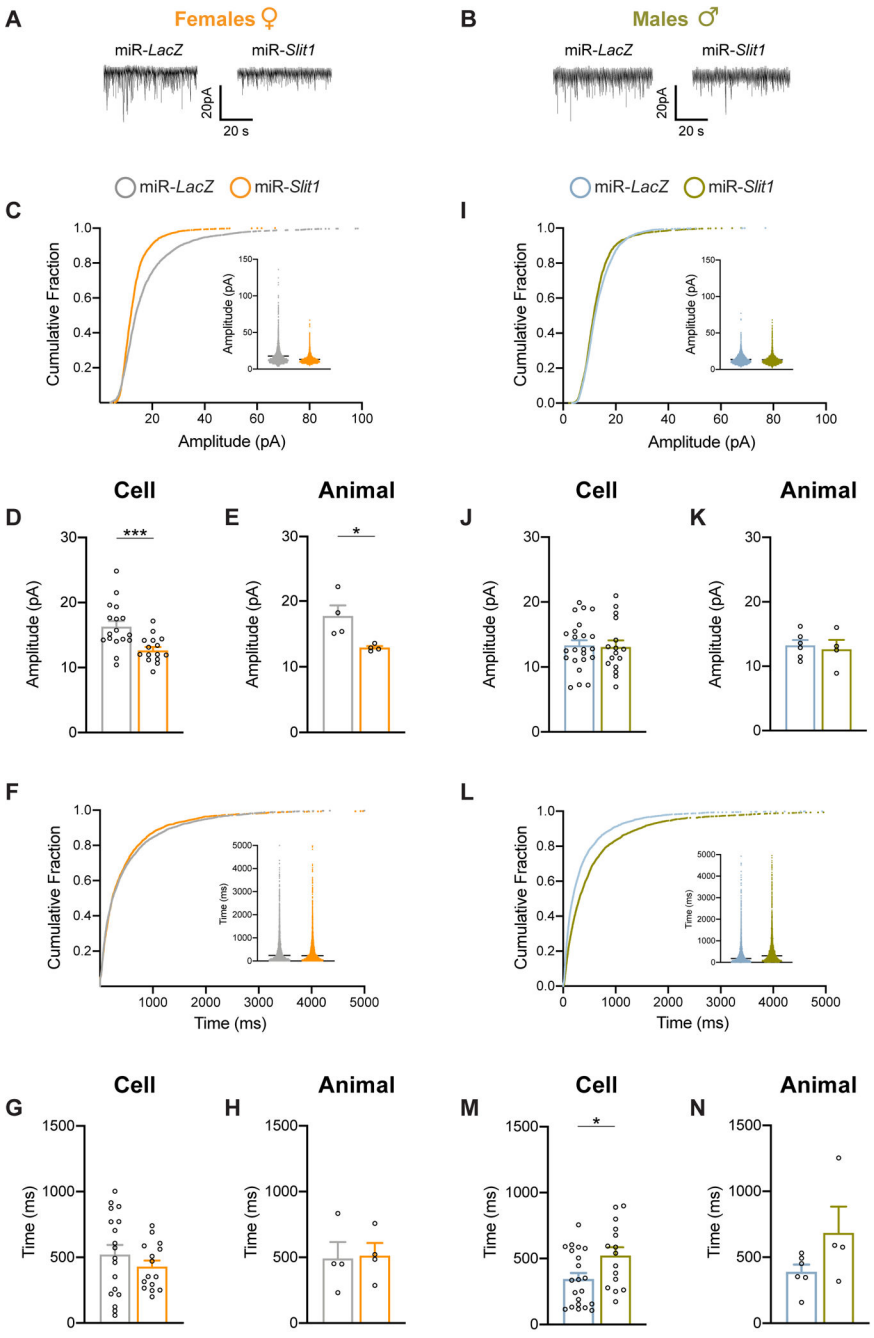

Figure 4. ***Slit1*** **KD modulates mEPSC amplitude in vmPFC pyramidal neurons of female mice.** **(A, B)** Representative membrane potential of pyramidal neurons in the vmPFC of female **(A)** or male **(B)** mice after *Slit1* or *LacZ* KD. **(C)** Cumulative curves and scatter plots for mEPSC amplitude of female mice. **(D, E)** Bar graphs indicate that *Slit1* KD decreased the amplitude of mEPSCs compared to miR-*LacZ* on a "per cell" (n=15-17 cells/group) **(D)** or "per animal" (n=4 animals/group) **(E)** basis. **(F)** Cumulative curves and scatter plots for mEPSC interevent interval of female mice. **(G, H)** *Slit1* KD in females had no effect on mEPSC interevent interval per cell **(G)** or per animal **(H)**. **(I)** Cumulative curves and scatter

plots for mEPSC amplitude of male mice. **(J, K)** *Slit1* KD in males had no effect on mEPSC amplitude per cell **(J)** or per animal **(K)**. **(L)** Cumulative curves and scatter plots for mEPSC interevent interval of male mice. **(M, N)** Bar graphs indicate that *Slit1* KD increased mEPSC interevent interval compared to miR-*LacZ* per cell (n=15-21 cells/group) **(M)**, but not per animal (n=4-6 animals/group) **(N)**. ***p<0.001.

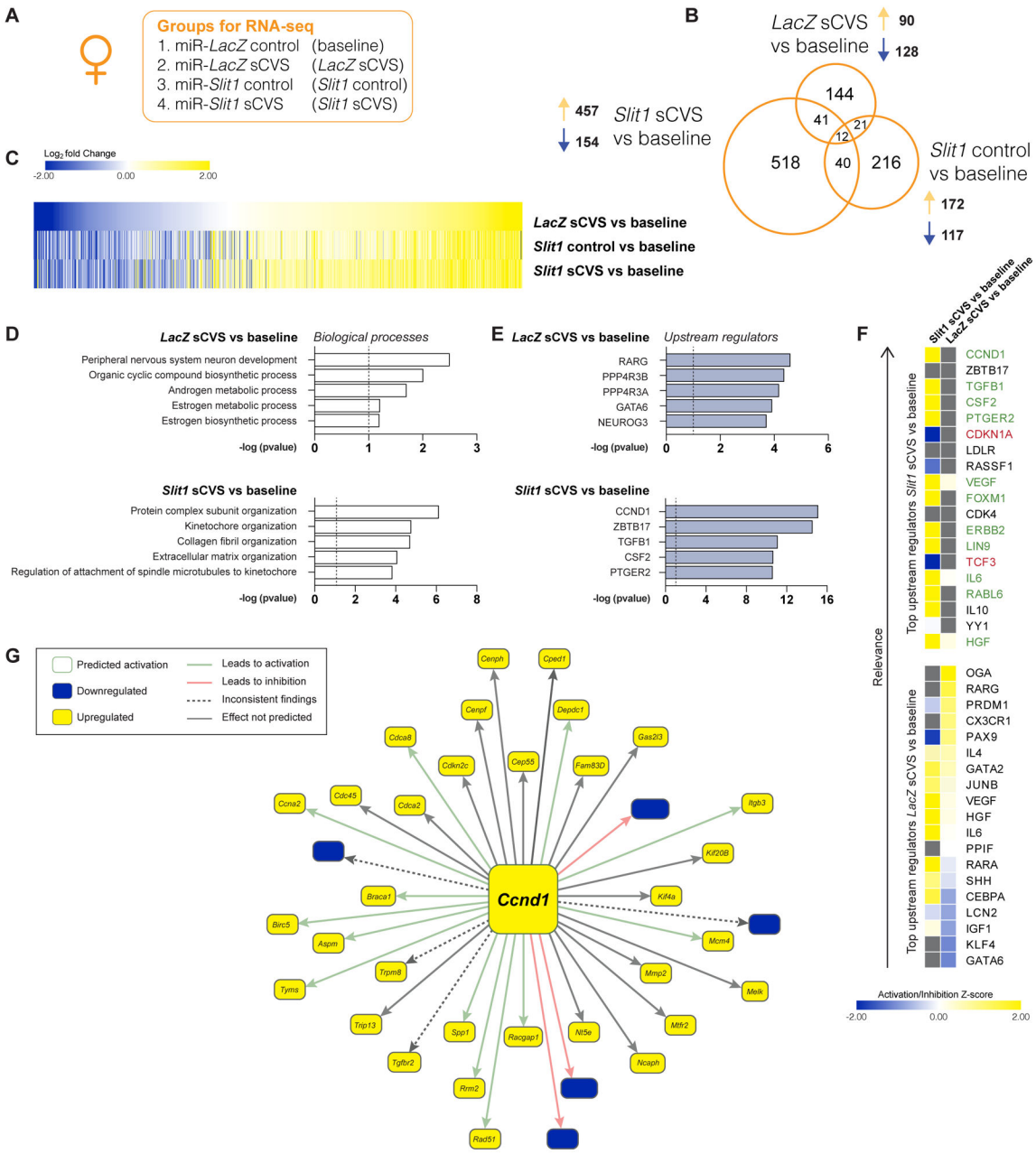

Figure 5. RNA-seq reveals transcriptional alterations in the vmPFC of female mice after *Slit1* KD that predict *Ccnd1* as an upstream regulator.

(A) List of experimental groups (n=7/group). **(B)** Venn diagrams showing the overlap in the list of differentially expressed genes (DEGs) between the groups (DEG cutoff: fold change >30% and p<0.05). **(C)** Union heatmap comparing DEG patterns between the *LacZ* sCVS vs. baseline (top lane), *Slit1* control vs. baseline (middle lane), or *Slit1* sCVS vs. baseline (bottom lane) groups. *Slit* KD augmented the effects of sCVS predominantly on upregulated genes. **(D)** Top enriched GO ontology terms from analysis of the DEGs following *LacZ* or *Slit1* KD and sCVS in female vmPFC compared to baseline. **(E)** Top predicted upstream regulators of DEGs regulated by sCVS after *LacZ* or *Slit1* KD compared to baseline. **(F)**

Top 20 upstream regulators and their activation or inhibition Z-score for *Slit1* sCVS (left panel) or *LacZ* sCVS (right panel) vs. baseline (green letters = activation; red= inhibition; grey letters = non). **(G)** Illustration of the gene network identified within the DEGs of the *Slit1* sCVS vs. baseline comparison, which is predicted to have *Ccnd1* as the top upstream regulator.

KEY RESOURCES TABLE

Resource Type	Specific Reagent or Resource	Source or Reference	Identifiers	Additional Information
Add additional rows as needed for each resource type	Include species and sex when applicable.	Include name of manufacturer, company, repository, individual, or research lab. Include PMID or DOI for references; use “this paper” if new.	Include catalog numbers, stock numbers, database IDs or accession numbers, and/or RRIDs. RRIDs are highly encouraged; search for RRIDs at https://scicrunch.org/resources.	Include any additional information or notes if necessary.
BLOCK-iT Pol II miR RNAi kit		Invitrogen	K493500	
RNAscope® Multiplex Fluorescent v2 Assay		Advanced Cell Diagnostics	323110	
mm-Slit1	Mus musculus	Advanced Cell Diagnostics	502491	Channel 1 Probe
mm-glutamic acid decarboxylase 2	Mus musculus	Advanced Cell Diagnostics	415071-C2	Channel 2 Probe
mm-vesicular glutamate transporter 2	Mus musculus	Advanced Cell Diagnostics	319171-C3	Channel 3 Probe
Alexa 488 Donkey anti-Chicken		Jackson ImmunoResearch	703546155	Secondary antibody IHC
ProLong™ Diamond Antifade Mountant		Thermo fisher scientific	P36961	
RNeasy Micro Kit (50)		Qiagen	74004	
iScript™ cDNA Synthesis Kit		Biorad	1708891	
TruSeq RNA CD Index Plate (96 Indexes, 96 samples)		illumina	20019792	
TruSeq Stranded Total RNA Library Prep Gold (48 samples)		illumina	20020598	
Agencourt AMPure XP, 60 mL		Beckman Coulter	A63881	
Agencourt RNAClean XP		Beckman Coulter	A63987	
RNase-Free DNase Set (50)		Qiagen	79254	
qPCR primers		IDT	Custom	